

PXS-T2R-014

**SPES-2 HOT PREOPERATIONAL TEST H-06
INADVERTENT ADS STAGE 1 ACTUATION
(WITH NO ADS STAGE 4)**

AP600 PROGRAM

JULY 1995

1.0 INTRODUCTION

This report describes and discusses the results of the SPES-2 hot preoperational test H-06, which was performed on December 18, 1993. Preoperational test H-06 simulated an inadvertent actuation of stage 1 of the ADS, at full power conditions. The key objectives of this test were to:

- Demonstrate the proper automatic actuation of components based on the setpoints described below.
- Demonstrate automatic reduction of the rod bundle power by the control system to simulate reactor trip from full power, post-trip power, decay heat, and heat loss compensation.
- Verify the sizing of the ADS flowpath orifices by observing that the SPES-2 primary system is depressurized in a manner similar to that expected in the AP600.

Test Description/Procedure

Hot preoperational test H-06 was performed with the facility initially operating at full pressure, and full scaled power and flow. The test was initiated by opening the ADS stage 1 isolation valve, which caused the primary system pressure to decrease, and resulted in the actuation of the reactor trip signal (R-signal) and safety injection signal (S-signal). All actuations subsequent to the opening of the ADS stage 1 isolation valve were performed automatically.

When the R-signal is actuated (PZR pressure = 1800 psia), the heater rod power is to be initially controlled to match the scaled integrated AP600 core heat output that occurs after an actual plant trip, as follows:

- Heater rod power was to be maintained at 100 percent until R-signal + 5.75 seconds.
- Heater rod power was then to be reduced to 20 percent of full power and maintained until R-signal + 14.5 seconds.
- Heater rod power was then to be controlled to match core decay heat versus time plus 110 kW (power will not exceed 20 percent of full power)

Note that the 110 kW of power was provided to compensate for the higher than scaled SPES-2 facility heat loss.

- The 110 kW of extra heater rod power for heat loss compensation was to be terminated when the ADS second stage isolation valve was opened

Additional actuations which were to occur when the R-signal was actuated included:

- SG steam isolation valves were to close at the R-signal.

When the S-signal is actuated (PZR pressure = 1700 psia), the following actuations were to occur:

- CMT CL balance line and discharge line isolation valves were to open at S-signal +2 and 8 seconds, respectively.
- SG feedwater lines were to close at S-signal + 2 seconds.
- RCPs were to be tripped at S-signal + 16.2 seconds.
- Pressurizer internal heaters were to be turned off at the S-signal.

In addition to the S- and R-signal based actuations the following additional actuations were specified:

- PZR external heaters were to be turned off when ADS Stage 1 was opened.
- PRHR HX discharge line isolation valve was to open on low SG narrow range level (0.15 m) + 45 seconds.
- ADS stage 2 isolation valve was to open when the level in either CMT was ≤ 60 percent.
- ADS stage 3 valve was to open when the level in either CMT was ≤ 50 percent.
- One out of two ADS stage 4 isolation valves was to open when the level in either CMT was ≤ 20 percent.

CMT balance line trace heaters were to be manually turned off.

Test Initial and Boundary Conditions

Table 1 provides a comparison of the specified and actual initial conditions for Test H-06. The initial condition values in the table were averaged over the 300 seconds preceding the test, i.e., opening of the ADS stage 1 valve. No measurements deviated from the specified tolerance sufficiently to have had a significant effect on the test objectives.

The actual heated rod bundle power versus time is provided in the data plot 1. The sequence of events that actually occurred in the test is shown in Table 2 and event timing is compared with the specified setpoints/times. As noted in this table, no flow through the ADS stage 4A occurred when the valve was opened. This was because a blank plate was installed in place of an orifice in the ADS

Stage 4A flowpath. The ADS stage 4B flowpath was also blocked since this path was to simulate the failure of the ADS stage 4B valve. Although having no ADS stage 4 flow had an impact on the test endpoint, the key objectives of the test were still satisfied since ADS Stages 1, 2 and 3 performance was observed. Although ADS Stage 4 performance could not be assessed, the ADS stage 4 for SPES-2 is ~ []^{a,b,c} times larger than scaled and was judged not to need verification prior to test S00103. ADS Stage 4 performance was assessed based on tests S00103 and S00203 prior to matrix test S00303.

Test Facility Configuration

Preoperational test H-06 was performed prior to the AP600 design changes to the ADS valve type, ADS valve opening setpoints, and deletion of the CMT PZR balance lines. Therefore, the SPES-2 facility configuration was somewhat different than that utilized in test S00303 and subsequent matrix tests. The key configuration differences for H-06, as compared to the matrix tests described in WCAP-14309, are outlined below:

- Two pressure balance lines were connected to the top of each CMT; the cold leg to CMT balance line and the PZR to CMT balance line.

The PZR to CMT balance line was routed from the top of pressurizer (actually from just upstream of the ADS valves) and Tee'd to the CMT cold leg balance line, just above each CMT. Each PZR to CMT steam balance line contained a check valve to prevent flow back to the PZR when/if ADS was actuated or if there was a PZR steam space break. The purpose of this line was to allow the CMT to drain with steam replacing the drained water when the RCPs were stopped, and if PZR level was low; independent of when the cold legs voided. The cold leg to CMT balance line also contained a normally closed isolation valve that opened after the S-signal.

- The size of the SPES-2 ADS stage 1 flowpath orifice was 1/395th of the two AP600 stage 1 globe valves each with []^{a,b,c} of flow area. (Matrix tests modeled two []^{a,b,c} flow areas).
- The size of the SPES-2 ADS stage 2 and 3 flowpath orifices were each 1/395th of two AP600 stage 2 or 3 gate valves, each with []^{a,b,c} of flow area. (Matrix tests modeled two []^{a,b,c} flow areas for stage 2 and 3.)
- The CMT level setpoints for actuating ADS-2 and 3 were 60 and 50 percent, respectively. (Matrix test ADS-2 and -3 setpoints were ADS-1 actuation plus 125 sec. and plus 245 sec., respectively).
- The SPES-2 cold leg to CMT balance lines were not orificed to match the scaled AP600 resistance. The low resistance cold leg to CMT balance lines were used in order to maximize

any tendency for localized steam condensation to occur at the PZR to CMT, and cold leg to CMT piping Tee; and therefore demonstrate if CMT draindown could be/would be delayed. In addition, the unorificed cold leg balance lines could drain in a more prototypic manner since no unprototypic steam water mixing at the reduced flow area of the orifice would occur. Note that the unorificed balance lines have very little effect on the CMT recirculation or draindown flow rate since most of the flow resistance is in the CMT discharge line. (These balance lines were orificed to match the AP600 scaled resistance and retested prior to matrix testing.)

- The CMT-A discharge line did not require an orifice to match the scaled AP600 resistance, since the check valve apparently had a high resistance. (This check valve was replaced, an orifice installed, and the line resistance was retested prior to matrix testing.)
- The accumulator injection lines both contained a 9.5 mm diameter orifice. However, based on this test these orifices were both replaced with a 4.86 mm orifice prior to matrix testing. Note that although accumulator flow rates were higher than expected in this test, this would have no major impact on the overall test results.
- The heat loss compensation used in this test was 110 kW. Based on subsequent analyses the heat loss compensation was increased to 150 kW for the matrix tests.

Test Results/Observations

This section describes some key test results and provides observations comparing this test and the results of the subsequent matrix tests.

Pressurizer Pressure

Plot 2 provides the pressurizer pressure (P-027P) versus time. As would be expected pressurizer pressure rapidly decreased when the ADS stage 1 valve was opened at time 0 seconds. This pressure decrease slowed when the primary system pressure decreased to []^{a,b,c}, the pressure corresponding to the saturation temperature of the fluid in the upper plenum/hot legs. However, the continued venting of fluid through the ADS stage 1 flowpath, combined with cold water addition by the CMTs and PRHR HX, resulted in continued steady depressurization of the primary system (~ []^{a,b,c} average depressurization rate) reaching ~ []^{a,b,c} when ADS stage 2 was actuated. The ADS stage 2 opening continued the primary pressure depressurization at approximately the same rate, and the primary system pressure reached []^{a,b,c}. After ADS stage 3 was opened, primary pressure decreased slowly, asymptotically reaching ~ []^{a,b,c} (measured at the top of the PZR) at []^{a,b,c} when IRWST injection began.

This H-06 depressurization appears less severe than the depressurization in Matrix Test S01211, where ADS was initiated at ~ 1800 psia. This is apparently due to the longer times between ADS stage 1, 2 and 3 actuations in this test.

CMT Injection

The CMT tank level instruments (L_A40E and L_B40E) and discharge flow (F_A40E and F_B40E) shown in Plots 33 and 38 indicate that the CMT performance was very similar in this H-06 test as compared to that observed in the matrix tests. When the CMT cold leg balance line and discharge line isolation valves were opened, both CMTs operated in a recirculation mode of operation for []^{a,b,c}. The CMTs then began to operate in a draindown mode, when the CLs began to drain and steam was able to flow to the top of the CMTs through the cold leg balance lines. This similarity was expected since no steam flow from the PZR to the CMT through the PZR to CMT balance line can/will occur when the ADS is actuated. This is because the top of the pressurizer is the low pressure point in the primary system with ADS operating (and RCPs off).

The CMT discharge flow was decreased when accumulator flow increased, since they share a common portion of the DVI line.

Accumulator Injection

The accumulator began to inject water at a low flowrate, into the primary system starting at []^{a,b,c}. This low injection flow rate continued until ADS-2 was opened at []^{a,b,c}, and flow rapidly increased to []^{a,b,c}. Accumulator flow again increased reaching []^{a,b,c} when ADS-3 opened at []^{a,b,c}. Accumulator flow rapidly decreased at []^{a,b,c} when the accumulators emptied. As noted above, this performance reflects the low injection line resistance that was installed at the time of this test; however, this would not cause a significant difference in the overall test results.

Overall Primary System Response

Plot 43 illustrates the integrated ADS mass flow as measured in the catch tank by instrument channel IF_030P, and Plot 44 provides the ADS flowrate derived from the catch tank data. From time 0 until ~ 100 sec. the ADS flowrate through the open ADS 1 flowpath was []^{a,b,c}. At this time the pressurizer rapidly filled with water (see Figure 1) and the ADS mass flow rate increased to []^{a,b,c}. As the primary system depressurized the void fraction of the fluid at the top of the pressurizer increased from []^{a,b,c} (see DP instruments DP-027P and 026P), and the ADS a flowrate decreased. During the time period from ADS-1 opening (time = 0) until the ADS-2 is opened, the ADS-1 flowrate averaged []^{a,b,c}. This mass loss is compensated for by the []^{a,b,c} average injection flow from the CMTs during this time, the small but increasing accumulator flow, and primary fluid from voided portions of the primary system. As shown in Plot 30 discussed below, the collapsed liquid level in the heater rod region actually increased from []^{a,b,c}

to []^{a,b,c} during this period. Note that Plot 30 shows the collapsed liquid level measured using DP instrument DP-000P which includes 2.43 ft. of water below the heated portion of the rod bundle (DP-005P) and 2.84 ft. of water/steam measured above the heated portion (DP-014P) which is converted to collapsed level in Plot 31.

When ADS-2 opened at []^{a,b,c}, the ADS flow increased sharply to []^{a,b,c} and averaged []^{a,b,c} until ADS-3 is opened. This mass loss was more than compensated by the accumulator injection and CMT injection flowrates, and the collapsed liquid level in the power channel increased to above the heated rod bundle (Plots 30 and 31). Concurrently the void fraction of the fluid near the top of the pressurizer, being discharged through the ADS, increases from []^{a,b,c} during this time period, and the overall level in the pressurizer decreased (see Figures 1 and 2).

The opening of the ADS-3 valve at []^{a,b,c}, resulted in another increase in ADS flow rate to []^{a,b,c}, however, the accumulator discharge flowrate again increased and maintained the water inventory in the heated rod region and upper plenum, while the collapsed level in the pressurizer increased and the void fraction of the fluid at the top of pressurizer decreased. The accumulators soon emptied at []^{a,b,c} and the total injection flow into the primary system, decreased to []^{a,b,c} from the two CMTs. The decreased injection flowrate is reflected by the heated rod region collapsed liquid level, which decreased to []^{a,b,c}; by the lower upper plenum fluid void fraction which increased from almost []^{a,b,c}; by the pressurizer collapsed liquid level which decreased from []^{a,b,c}; by the void fraction of the fluid at the top of the pressurizer which increase from []^{a,b,c}; and by a sharp decrease in the ADS flowrate to []^{a,b,c}.

Because the ADS-4A flowpath was inadvertently blocked no additional venting of the primary system was provided when the CMT-A level reached 20 percent at []^{a,b,c}, and injection flow from the IRWST was not immediately available. However, the CMTs continued to deliver water: with CMT-B flow decreasing from []^{a,b,c} lbs/sec at []^{a,b,c} when it emptied. CMT-A continued to deliver water until []^{a,b,c}, but did not completely empty. Both CMTs refilled slightly at []^{a,b,c} (when there was no injection flow from the IRWST) and both CMTs re-empty after refilling (see Plots 33 and 38).

As shown in Plot 40, flow from the IRWST via both the two IRWST injection lines initiated at []^{a,b,c}. The IRWST flow quickly increased to []^{a,b,c} per line which, combined with the CMT flow, corresponded closely with the mass being vented via the ADS-1, 2, 3 flowpaths. This was reflected by a small increase in the heater rod bundle collapsed liquid level. Note, however, that a steady IRWST flow rate was not established; but flow oscillated with a []^{a,b,c} period with substantial, simultaneous flow variations in both injection paths. Since the IRWST injection soon becomes the predominant source of injection to the primary system (CMT-B empties, and CMT-A flow is rapidly decreasing); the rod bundle collapsed level also oscillates. The same is true for the collapsed level measured in the lower upper plenum shown in Plot 30, and for the collapsed liquid

level in the PZR shown in Figure 1. The annular downcomer levels and hot leg levels also increased/decreased (Plots 24-27 and Plots 20 and 21 respectively) in conjunction with IRWST flow. Both the lower upper and upper upper plenum levels and PZR level showed a marked increase following the initiation of IRWST flow, until []^{a,b,c}

As shown in Plot 40, the IRWST injection flow although oscillating began to decrease at []^{a,b,c} and essentially stopped at []^{a,b,c}. At []^{a,b,c} the IRWST flow is again initiated, quickly increased reaching []^{a,b,c} peak flow through each injection line with large oscillations. Flow began to decrease at []^{a,b,c} and again essentially stopped with subsequent oscillations from []^{a,b,c}. Again at []^{a,b,c} oscillating flow began and reached peak flow rates of []^{a,b,c} per injection line at []^{a,b,c}, and continued until the test was terminated at []^{a,b,c}. It can be generally observed from comparing the IRWST flow versus time with Plots 30, 31, and Figure 1 that the IRWST injected when the average collapsed liquid levels in the heater rod bundle, lower-upper plenum, and pressurizer are at their minimum level (maximum void fraction) and stopped injecting when the levels were at their maximum (minimum void fraction). This overall change in water level (void fraction) was also accompanied by shorter duration oscillations of large magnitude in measured level that have a period of []^{a,b,c} like the IRWST flow oscillations. These oscillations are most apparent in the overall PZR collapsed level where the individual oscillations range from []^{a,b,c} of measured level ([]^{a,b,c} void fraction) change. In addition to the change in overall level and void fraction, the discharge of mass from the PZR via the ADS-1, 2, 3 essentially stopped when IRWST flow stopped. Note that this was when the CMTs were partially refilling and at the same time providing injection flow.

The initiations and stops in IRWST flow can be seen to result from the primary system overall pressure. The observed pressure at the bottom of the power channel downcomer (P-001P) shown in Figure 3 has been adjusted by subtracting the elevation head of water in the downcomer to obtain the actual pressure at the DVI nozzle inlet to the annular downcomer. It can be seen that the IRWST began to inject at []^{a,b,c} when the primary pressure at the DVI nozzle was []^{a,b,c}. IRWST flow then stopped at []^{a,b,c} when the pressure increased to []^{a,b,c}, started at []^{a,b,c} when this pressure decreased to []^{a,b,c}, stopped at []^{a,b,c} when pressure increases to []^{a,b,c}, and restarted at []^{a,b,c} when pressure decreases to []^{a,b,c} again.

As evidenced by the small changes in primary pressure associated with initiating and stopping IRWST flow discussed above, very small primary system pressure changes would cause the IRWST flow oscillations. The fluid temperatures in Plots 5-8 clearly show that the saturated hot leg fluid reaches the SG inlet after IRWST injection started and that some fluid reached the SG tubes. Since the SG's are still very hot, this fluid was flashed and this appears to be the source of small pressure changes. For example, Plot 7 shows that the temperature in the lower part of SGA tube(s) (T-A05P) decreases from ~ 450°F to ~ 250°F (the primary system saturation temperature) at ~ 2450 seconds. This time corresponds to when the first oscillation in the IRWST flow is observed.

TABLE 1
INITIAL TEST CONDITIONS FOR PRE-OPERATIONAL TEST H-06

Parameter (Instruments)	Specified for Matrix Test	Actual	Comment
Rod Power (W-00P)	4910 ± 100 kW		
Pressurizer Pressure (P-027P)	2241 ± 29 psia		
Average HL Temperature (T-A03PO/T-A03PL/ T-B03PO/T-B03PL)	602.2 ± 9 °F		
Reactor Vessel (Core) Inlet Temperature (T-003P)	538.0 ± 9 °F		
Core Flowrate (F_003P)	51.54 ± 0.55 lbm/sec.		
Cold Leg Flowrate (F_A01P/F_A02P/F_B01P/ F_B02P)	12.85 ± 0.22 lbm/sec.		
DC-UH Bypass Flowrate (F_014P)	0.40 ± 0.11 lbm/sec.		
Pressurizer Level (L_010P)	12.24 ± 1.25 ft.		
Accumulator Level (L_A20E/L_B20E)	7.55 ± 0.36 ft		
Accumulator Water Temperature (T-A22E/ T-B22E)	68 ± 9 °F		
Accumulator Pressure (P-A20E/P-B20E)	711 ± 14.5 psia		
IRWST Level (L_060E)	27.9 ± .32 ft		

a.b.c

**TABLE 1 (Cont.)
INITIAL TEST CONDITIONS FOR PRE-OPERATIONAL TEST H-06**

Parameter (Instruments)	Specified for Matrix Tests	Actual	Comment
IRWST Water Temperature (T-063E)	$68 \pm 9^{\circ}\text{F}$		
PRHR Supply Line Temperature (T-A82E)	$230.5 \pm 22.5^{\circ}\text{F}$		
UH Average Temperature (T-016P)	$511 \pm 9^{\circ}\text{F}$		
PR to CMT Balance Line Temperature (T-A28P/ T-B28P)	$644 \pm 45^{\circ}\text{F}$		
CL Balance Line Temperature (T-A142PL/ T-B142PL)	$> 329^{\circ}\text{F}$		
CMT Level (L_A40E/ L_B40E)	$20.5 \text{ ft.} \pm 0.1 \text{ ft}$		
CMT Temperature (T-A411E/T-B411E)	$68 \pm 9^{\circ}\text{F}$		
SG Level (L_A20S/L_B20S)	$4.92 \pm 0.49 \text{ ft}$		
SG MFW Temperature (T-A01S/T-B01S)	$432 \pm 13^{\circ}\text{F}$		
SG Pressure (P-A04S/ P-B04S)	$711 \pm 29 \text{ psia}$		

a,b,c

TABLE 2
SEQUENCE OF EVENTS FOR PRE-OPERATIONAL TEST H-06

Event	Specified	Instrument Channel	Actual Time (Sec.)
ADS Stage/Valve Opened	0	Z_001PC/Z_001PO	a.b.c
Reactor Trip Signal "R"	P = 1800 psia	P-027P	
MSL IV Closed	R Signal	Z_A04SO/Z_A04SC	
		Z_B04SO/Z_B04SC	
Rod Power Reduction	R Signal + 5.7 sec.	W_00P	
S Signal	P = 1700 psia	P-027P	
CMT BL IV Opened	S Signal	Z_A45PC/Z_A45PO	
		Z_B45PC/Z_A045PO	
CMT Disch. IV Opened	S Signal + 8 sec.	Z_A40EC/Z-A40EO	
		Z_B40EC/Z-B40EO	
PRHR HX IV Opened	LO NR SG level + 45 sec.	Z_A81EC/Z_A81EO	
MFW IV Closed	S Signal	Z_A02S0/Z_A025C	
		Z_B02S0/Z_B025C	
Reactor Coolant Pumps Tripped	S Signal + 16.2 sec.	DP-A00P	
		DP-B00P	
Accumulator Delivery Initiation	P-027P = 710 psia		
		F_A20E/F_B20E	
ADS 2 Opened	CMT Level 60%	L_B40E	
		Z_002PC/Z_002PO	
Heat Loss Compensation Off	ADS 2 Actuation	W_OOP	
ADS 3 Opened	CMT Level 50%	L_B40E	
		Z_003PC/Z_003PO	
ADS 4 A Opened (Note: flowpath blocked)	CMT Level 20%	L_B40E	
		Z_A04PC/Z_A04PO	

TABLE 2 (Cont.)
SEQUENCE OF EVENTS FOR PRE-OPERATIONAL TEST H-06

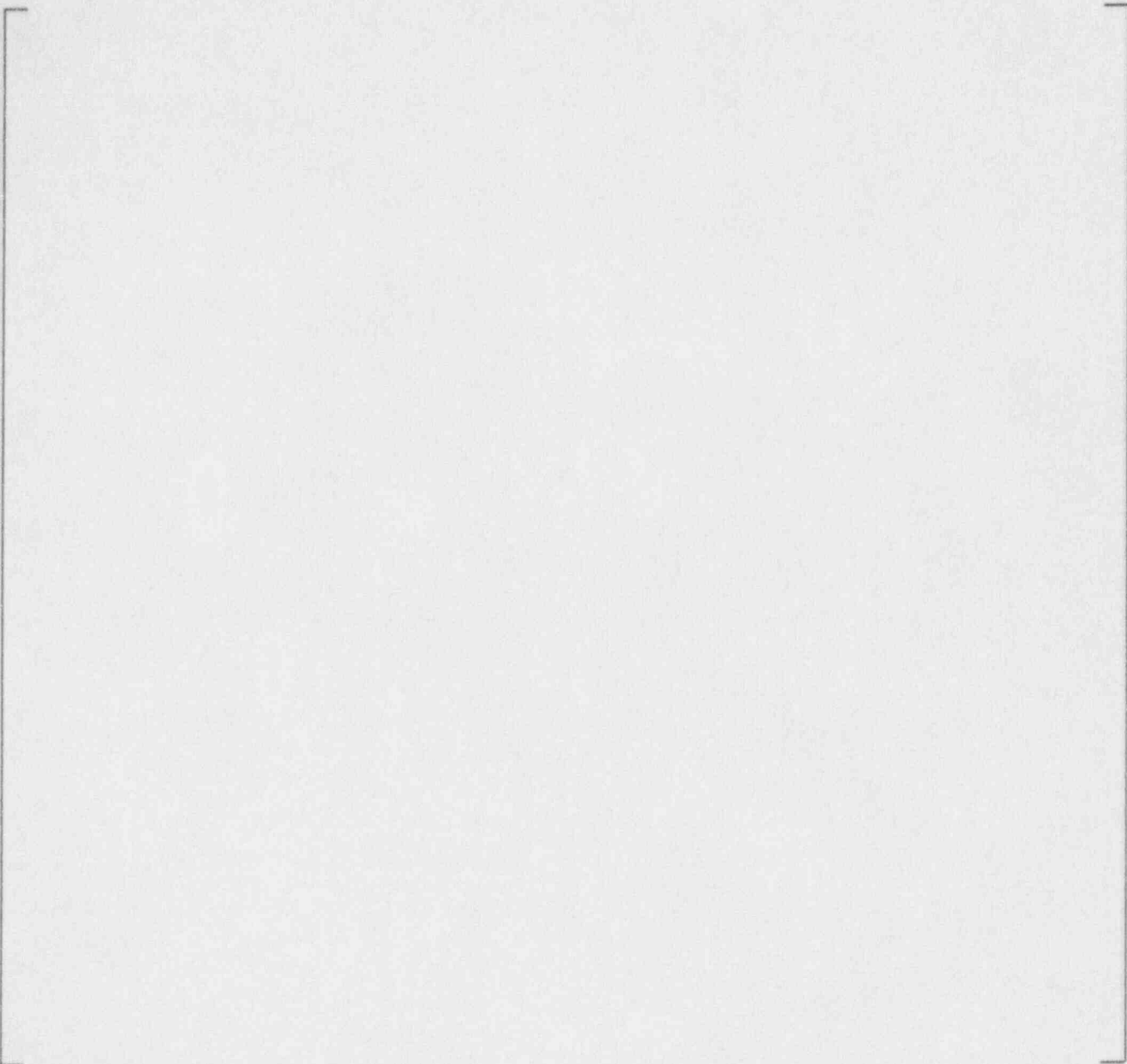
Event	Specified	Instrument Channel	Actual Time (Sec.)
IRWST Injection Start/Stop		F_A60E/F_B60E	[]

a,b,c

TABLE 3
SPES-2 INSTALLED ORIFICES FOR TEST H-06

Location	Diameter (mm)	Thickness (mm)
ADS-1	4.99	12
ADS-2	10.79	12
ADS-3	10.79	12
ADS-4A	blocked*	N/A
ADS-4B	blocked to simulate single failure	N/A
CMT-A injection line	no orifice	N/A
CMT-B injection line	5.7	5.5
CMT-A cold leg bal. line (2 orif.)	no orifice	N/A
CMT-B cold leg bal. line (2 orif.)	no orifice	N/A
Accumulator-A injection line	9.5	7.3
Accumulator-B injection line	9.5	7.3

* Blank plate inadvertently installed



a.b.c



a.b.c



a.b.c

**TABLE 4
SPES-2 TEST H-06 PLOT PACKAGE
CHANNEL LIST BY COMPONENT**

COMPONENT	CHANNEL	UNITS	PLOT	COMMENT
ACCA	F_A20E	lbm/sec.	39	
ACCA	L_A20E	ft.	34	
ACCB	F_B20E	lbm/sec.	39	
ACCB	L_B20E	ft.	34	
ADS 1, 2, & 3	IF30f1w	lbm/sec.	44	Flow rate derived from 1F030P
ADS 1, 2, & 3	IF030P	lbm	43	Catch tank
ADS 4 & SG	IF40f1w	lbm/sec.	44	Flow rate derived from 1F040P
ADS 4 & SG	IF040P	lbm	43	Catch tank
ANND	DP-A021P	psi	24	To cold leg-A1
ANND	DP-A022P	psi	25	To cold leg-A2
ANND	DP-B021P	psi	26	To cold leg-B1
ANND	DP-B022P	psi	27	To cold leg-B2
BREAK LINE	IF05f1w	lbm/sec.	44	Flow rate derived from 1F005P
BREAK LINE	IF005P	lbm	43	Catch tank
CLA	DP-A001P	psi	24	To cold leg-A1
CLA	DP-A002P	psi	25	To cold leg-A2
CLA	DP-A09P	psi	22	Pump suction
CLA	T-A10P	°F	11	Steam generator outlet
CLA1	F-A01P	lbm/sec.	36	
CLA1	T-A021PL	°F	13	Downcomer inlet
CLA1	T-A11P	°F	11	Pump outlet
CLA2	F_A02P	lbm/sec.	36	
CLA2	T-A022PL	°F	13	Downcomer inlet
CLB	DP-B001P	psi	26	To cold leg-B1
CLB	DP-B002P	psi	27	To cold leg-B2
CLB	DP-B09P	psi	23	Pump suction
CLB	T-B10P	°F	12	Steam generator outlet
CLB1	F_B01P	lbm/sec.	36	
CLB1	T-B021PL	°F	14	Downcomer inlet

TABLE 4 (Cont.)
SPES-2 TEST H-06 PLOT PACKAGE
CHANNEL LIST BY COMPONENT

COMPONENT	CHANNEL	UNITS	PLOT	COMMENT
CLB1	T-B11P	°F	12	Pump outlet
CLB2	F-B02P	lbm/sec.	36	
CLB2	T-B022PL	°F	14	Downcomer inlet
CMTA	F_A40E	lbm/sec.	38	
CMTA	L_A40E	ft.	33	
CMTA	T-A401E	°F	15	Top (242.25 in.)
CMTA	T-A403E	°F	15	216.75 in.
CMTA	T-A405E	°F	15	191.25 in.
CMTA	T-A407E	°F	15	165.75 in.
CMTA	T-A409E	°F	15	140.25 in.
CMTA	T-A411E	°F	15	114.75 in.
CMTA	T-A413E	°F	15	89.25 in.
CMTA	T-A415E	°F	15	63.75 in.
CMTA	T-A417E	°F	15	38.25 in.
CMTA	T-A420E	°F	15	Bottom (0 in.)
CMTB	F_B40E	lbm/sec.	38	
CMTB	L_B40E	ft.	33	
CMTB	T-B401E	°F	16	Top (242.25 in.)
CMTB	T-B403E	°F	16	216.75 in.
CMTB	T-B405E	°F	16	191.25 in.
CMTB	T-B407E	°F	16	165.75 in.
CMTB	T-B409E	°F	16	140.25 in.
CMTB	T-B411E	°F	16	114.75 in.
CMTB	T-B413E	°F	16	89.25 in.
CMTB	T-B415E	°F	16	63.75 in.
CMTB	T-B417E	°F	16	38.25 in.
CMTB	T-B420E	°F	16	Bottom (0 in.)
CVCS	F-001A	psi	42	
DVIA	T-A00E	°F	13	

**TABLE 4 (Cont.)
SPES-2 TEST H-06 PLOT PACKAGE
CHANNEL LIST BY COMPONENT**

COMPONENT	CHANNEL	UNITS	PLOT	COMMENT
DVIB	T-B00E	°F	14	
HLA	DP-A04P	psi	20	
HLA	T-A03PL	°F	5	Vertical, near power channel
HLA	T-A03PO	°F	5	Horizontal, near power channel
HLA	T-A04P	°F	5	Near steam generator inlet
HLB	DP-B04P	psi	21	
HLB	T-B03PL	°F	6	Vertical, near power channel
HLB	T-B03PO	°F	6	Horizontal, near power channel
HLB	T-B04P	°F	6	Near steam generator inlet
IRWST	F_A60E	lbm/sec.	40	
IRWST	F_B60E	lbm/sec.	40	
IRWST	L_060E	ft.	32	
IRWST	T_061E	°F	17	Bottom Tank
IRWST	T_062E	°F	17	Bottom Tube
IRWST	T_062EA	°F	17	Bottom Tube
IRWST	T_063E	°F	17	Middle Tube
IRWST	T_063EA	°F	17	Middle Tube
IRWST	T_064E	°F	17	Top Tube
IRWST	T_064E(-3)	°F	17	Top Tube (average of 3)
IRWST	T-06'E(-4)	°F	17	Top Tank (average of 4)
NRHRA	F-A00E	psi	42	
NRHRB	F-B00E	psi	42	
PC	W_00P	kW	1	
PC-HB	L_000P	ft.	30	Heater bundle
PC-HR	TW018P20	F	3	Heater rod
PC-HR	TW018P48	F	3	Heater rod
PC-HR	TW020P87	°F	3	Heater rod
PC-UH	T-016P	°F	4	Upper head
PC-UP	L_A15P	ft.	30	Bottom of upper plenum
PC-UP	L_A16P	ft.	31	Top of upper plenum

**TABLE 4 (Cont.)
SPES-2 TEST H-06 PLOT PACKAGE
CHANNEL LIST BY COMPONENT**

COMPONENT	CHANNEL	UNITS	PLOT	COMMENT
PC-UP	T-015P	°F	4	Upper plenum
PC_UH	L_017P	ft.	31	Upper head
PC_UP	L_A14P	ft.	31	Above top of the active fuel
PRHR	DP-A81AE	psi	29	Supply line inverted U-tube
PRHR	DP-A81BE	psi	29	Supply line inverted U-tube
PRHR	DP-A81E	psi	28	Supply line
PRHR	DP-A82E	psi	28	Heat exchanger
PRHR	DP-A83E	psi	28	Return line
PRHR	F_A80E	lbm/sec.	37	Return line
PRHR	T-A82E	°F	19	Inlet
PRHR	T-A83E	°F	19	Exit
PZR	L_010P	ft.	32	
PZR	P-027P	psia	2	
PZR	T-026P	°F	18	487 in.
SGA	DP-A05P	psi	20	Hot side
SGA	DP-A06P	psi	20	Hot side
SGA	DP-A07P	psi	22	Cold side
SGA	DP-A08P	psi	22	Cold side
SGA	F_A01S	lbm/sec.	41	Main SLA feed
SGA	F_A20A	lbm/sec.	41	Secondary SLA feed
SGA	L_A10S	ft.	35	Overall level
SGA	P-A04S	psia	2	Secondary system
SGA	T-A01S	°F	10	MFW-A
SGA	T-A05P	°F	7	Hot side
SGA	T-A05S	°F	9	Hot side - riser
SGA	T-A06P	°F	7	Hot side
SGA	T-A08P	°F	11	Cold side
SGA	TW-A06S	°F	7	Hot side
SGB	DP-B05P	psi	21	Hot side

**TABLE 4 (Cont.)
SPES-2 TEST H-06 PLOT PACKAGE
CHANNEL LIST BY COMPONENT**

COMPONENT	CHANNEL	UNITS	PLOT	COMMENT
SGB	DP-B06P	psi	21	Hot side
SGB	DP-B07P	psi	23	Cold side
SGB	DP-B08P	psi	23	Cold side
SGB	F_B01S	lbm/sec.	41	Main SLB feed
SGB	F_B20A	lbm/sec.	41	Secondary SLB feed
SGB	L_B10S	ft.	35	Overall level
SGB	P-B04S	psia	2	Secondary system
SGB	T-B01S	°F	10	MFW-B
SGB	T-B05P	°F	8	Hot side
SGB	T-B05S	°F	9	Hot side - riser
SGB	T-B06P	°F	8	Hot side
SGB	T-B07P	°F	8	U-tube top
SGB	T-B08P	°F	12	Cold side
SGB	TW-B06S	°F	8	Hot side
SL	T-020P	°F	18	Surge line near pressurizer
TDC	DP-001P	psi	25,26	Top
TDC	DP-002P	psi	24,25,26,27	Bottom
TDC	T-001PL	°F	13,14	Top
TDC	T-003P	°F	13,14	Bottom
TSAT-PZR		°F	18	Based on P-027P
UH-TSAT		°F	4	Based on P-017P

Plots 1 through 44 contain proprietary information and have been deleted.